

A MULTISCALE MODEL OF THE ALUMINIUM LAYER AT THE REAR SIDE OF A SOLAR CELL

T. van Amstel¹, V. Popovich² and I.J. Bennett¹

¹ECN Solar Energy, P.O. Box 1, 1755 ZG Petten, The Netherlands

²Department of Materials Science and Engineering, Delft University of Technology, Mekelweg 2, 2628 CD Delft, The Netherlands

Phone: +31 224 564847; Fax: +31 224 568214; email: vanamstel @ecn.nl

ABSTRACT: In order to achieve faster time to market for new innovations and to optimize existing manufacturing processes it is becoming increasingly important to develop models that allow for the design and optimization of new cells and modules. In this article a thermo-mechanical bowing model of a solar cell after firing is described. The model integrates the thermo-mechanical behaviour of the layers at the rear of the cell to allow bowing of the cell to be predicted. Most commercially manufactured solar cells consist, apart from a p-type silicon bulk, of a number of layers: silver, silicon-nitride, BSF and rear-side aluminium. The silicon, silver, silicon-nitride, BSF and eutectic Al-silicon rear-side layers can be accurately described using standard modelling techniques. The Al bulk layer can best be modelled as a composite material. A Mori-Tanaka homogenisation method was used in combination with detailed finite element models of the Al microstructure to predict the mechanical response of the Al layer. This composite modelling approach allows the mechanics of the Al microstructure to be related to the effect of Al on cell bowing. Microstructural features include morphology, inclusion size, aspect ratio distribution and mechanical properties of the inclusions in the Al layer. The model can also be used to predict the Al microstructure based on measurements of cell bowing. Furthermore it is shown that when plastic behaviour is incorporated that final bowing is determined by the flow stress and hardening behaviour of the eutectic and Al bulk layer. The Young's moduli of the eutectic and Al bulk layer, thermal expansion coefficients and temperature change during the firing process do not directly affect final bowing.

Keywords: Modelling, finite element method, bowing, silicon solar cell

1. INTRODUCTION

The reduction in time to market can be achieved by building analytical and computer models that capture the essence of certain processes and use these models to make and set up new product requirements and designs.

Many industrial solar cell processes use p-type multicrystalline wafer material. During the firing process wafers that have been textured, doped, silicon nitride coated and screen printed with silver and Al pastes are fired at approximately 800 °C for a short time. This is followed by cooling to room temperature. The purpose of this process is twofold: 1) to create electrical contacts between the metal components in the screen-printed pastes and the silicon wafer and 2) to passivate the rear-side of the cell with a back-surface field (BSF) formed by diffusion of Al into the p-type silicon bulk of the cell, so minimizing electron-hole pair recombination. However, firing process creates residual stresses within the cell due to mismatch of thermal expansion coefficients and different mechanical behaviour of the materials used in the metallic contacts. The wafer bows and forms a convex or concave body upon cooling, which mechanically loads the cell and may cause fracture.

As the thickness of silicon wafers is reduced, cell bowing becomes a major problem during different processing steps. To further reduce costs by using

ever thinner wafers, whilst maximizing yield and efficiency, it is becoming increasingly important to understand the firing process from a thermo-mechanical point of view.

Recently, a first generation of finite element models to achieve these goals was developed [1]. In this article a second generation of firing models based on the latest materials insight is presented to further improve our understanding of the firing process. A thermo mechanically uncoupled solution is used, wherein the temperature is homogeneously predefined in space. The behaviour of the Al bulk rear-side layer is predicted on the basis of Mori Tanaka and finite element homogenization of the microstructure. The different material layers present after the firing process are modelled both thermodynamically and kinematically.

The firing models exhibit both non linear geometric and non linear material behaviour. The non linearity of the material behaviour is seen in that final bowing is not determined by the eutectic and Al bulk layer young's modulus, temperature change during the firing process and thermal expansion coefficients, but by the flow stress (the stress that causes the material to deform plastically) and hardening (the possible change of flow stress due to plastic deformation) behaviour of the eutectic and Al bulk layer.

The flow stress in the Al bulk layer can be predicted using both the firing model and the Al bulk

homogenization models. It is shown in this article that the predictions are in agreement when the Al bulk layer for the most part consists of Al particles. This is confirmed by direct computed tomography and XRD measurements of the bulk layer.

On the basis of this model it should be possible to design a new low bow aluminium paste as well as to determine mechanical limits of the solar cell, with the aim of reducing yield losses during cell and module manufacture.

2. OBSERVING THE FIRING PROCESS

It is known from experimental investigation that during the heating up phase of the firing process the Al paste on the rear side of the wafer melts. Furthermore it is known that a percentage of Al melt adjacent to the silicon wafer creates a liquid eutectic layer. Depending on processing times and temperatures the thicknesses of the eutectic and Al liquid layer varies. As the eutectic mixture cools down during the cooling phase of the firing process and since the Si content has to decrease following the liquidus curve in the Al-Si phase diagram an epitaxial BSF layer is grown with an excess of silicon from the eutectic mixture [2]. Also according to the phase diagram the Al bulk solidifies at 660 °C, followed at 570 °C by the solidification of the eutectic layer. The result at room temperature is a layer stack of silver at the front side of the cell, silicon bulk, BSF, eutectic and Al bulk. The BSF, eutectic and Al bulk material are known as the back surface layers. Figure 1 shows a typical SEM cross section picture of a fired cell showing 5 distinct layers. Polished and etched cross sections images were used to measure the BSF and eutectic layer thickness.

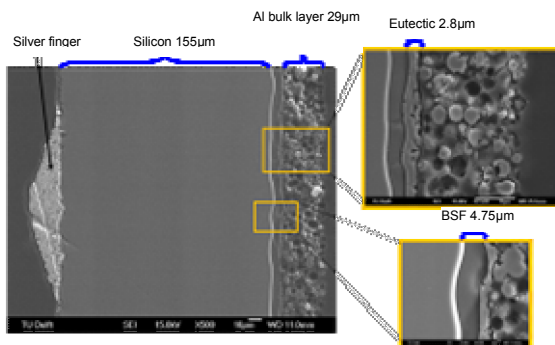


Figure 1: Polished SEM cross section of a fired cell consisting of an Ag finger, Si wafer, the BSF layer, the eutectic layer and an Al bulk layer.

3. BOWING

For a two layer stack, as shown in Figure 2, using plain strain conditions bowing can be described analytically.

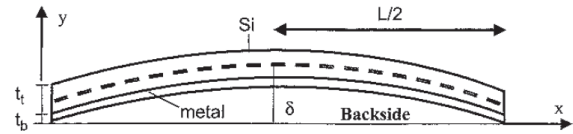


Figure 2: A stack of consisting of silicon and a metal. The stack endures bowing due to thermal expansion mismatch and temperature change.

If the stack consists of a silicon top layer and an Al bottom layer and when plastic behaviour for the Al layer is used, then the maximum bowing can be described by Equation 1. This equation can be derived by formulating mechanical equilibrium for the two layer stack after cooling and assuming plastic behaviour for the metal bottom layer.

$$\delta = \frac{3}{4} L^2 \frac{t_b}{t_t^2} \frac{\sigma_{Al,flow,eff}}{E_{si}} \quad \text{Equation 1}$$

Where: L stands for length, t for thickness, E for Young's modulus, $\sigma_{Al,flow,eff}$ stands for the effective flow stress at room temperature of the Al bottom layer and δ for maximum bowing. The subscripts t and b stand for top and bottom. The above equation shows that the final bowing is only dependant on the effective flow stress with respect to the bottom layer. This means that material parameters such as the young's modulus and thermal expansion coefficient of the bottom layer do not influence the final bowing if the hardening of the bottom layer is negligible. The problem becomes focussed on finding realistic effective flow stresses for the Al bulk pastes after firing. The next section shows homogenization results that allow for the prediction of such effective flow stresses.

4. HOMOGENIZATION

In this section the macroscopic mechanical response of the Al bulk microstructure is explored. It is known from the analytical bowing description, which includes plastic behaviour, that to approximate the bowing after firing only the mechanical properties at room temperature are needed. This limits the scope to finding the effective flowstress for the Al bulk microstructures at room temperature.

Two different homogenization strategies are presented to describe the Al bulk layer: detailed finite element (FE) homogenization and the Mori Tanaka (MT) homogenization method. The results of both strategies are compared.

Figure 2 shows a draft model of the material composition of a solar cell cross-section after the firing process [3].

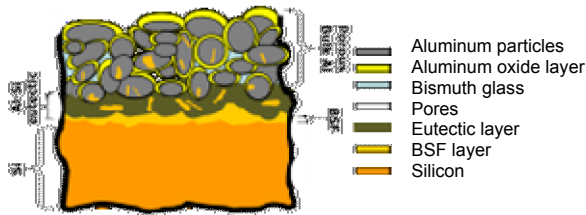


Figure 3: A draft model of a solar cell cross-section , showing the material build-up, after the firing process.

The Al bulk is composed of Al particles, bismuth glass, Al oxide and pores. This Al bulk composition can vary. Therefore a range of possible compositions is homogenized to predict its behaviour. A bracket notation to indicate the volume fractions for each composition is introduced as follows: (Al volume fraction : bismuth glass volume fraction : pores volume fraction : if present skin volume fraction). The following subsections describe the modelling results for different volume percentages of Al.

4.1 Composition with 40 volume percent of aluminium

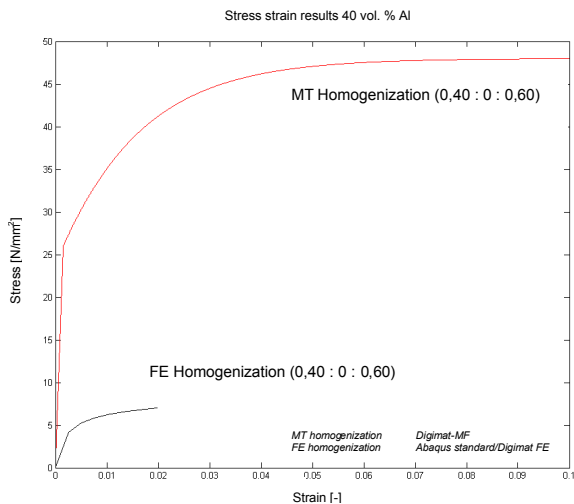


Figure 4: Stress strain results from the FE (lower curve) and MT (upper curve) homogenization strategies for 40 vol.% Al

Two observations can be made from these simulations:

1) A Large difference is predicted by the MT homogenization and the FE homogenization. These differences can be explained, since the MT homogenization assumes that all the Al deforms, by the occurrence of localized deformation as indicated by the localized stress shown in Figure 5.

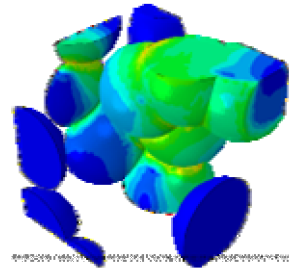


Figure 5: Predicted localized stresses by the finite element homogenization method.

2) The predicted effective flowstress in the range of 5 to 7 Newton per square millimeter is significantly lower than that of solid Al which is 72 Newton per square millimeter and higher.

4.2 Compositions with 55 volume percent of aluminium

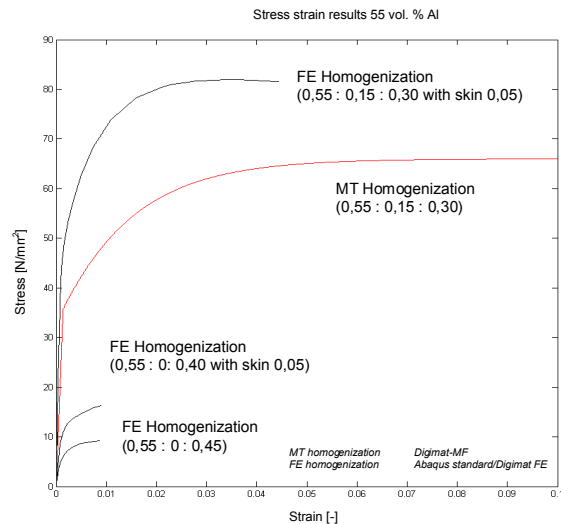


Figure 6: Stress-strain results from the FE (black) and MT (red) homogenization strategies for 55 vol.% Al. Also a simulation with an added skin to the composition is shown. The skin is defined as Al oxide surrounding the Al particles.

The FE results indicate an effective flow stress of 6 to 15 Newton per square millimeter for compositions that only consists of Al. For compositions that consist of 15 volume percent of bismuth silicon oxide and 55 volume percent of Al significantly higher flow stresses are predicted. Also the FE simulation show the influence of adding a skin to the composition. According to the simulations this influence is quite significant, a shift of about 10 Newton per square millimeter for 5 volume percent of extra skin material.

4.3 Compositions with 70 volume percent of aluminium

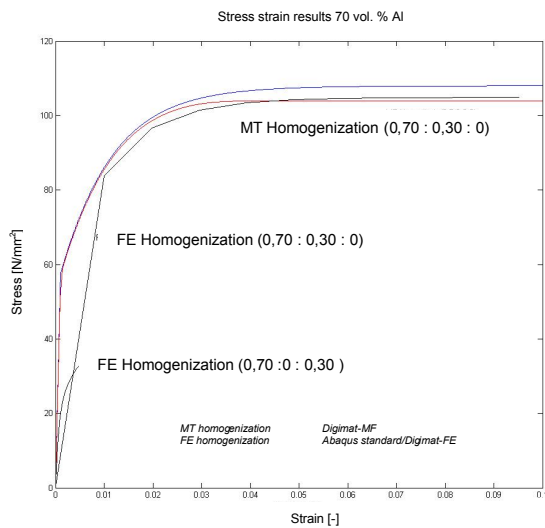


Figure 7: Stress strain results from the FE (black) and MT (red and blue) homogenization strategies for 70 vol.% Al. The blue line indicates a reverse MT homogenization.

For compositions consisting of 70 volume percent Al and 30 volume percent of bismuth silicon oxide the FE and MT homogenization methods make similar predictions. This indicates that the spatial size of the FE models used for the homogenization is sufficient. Furthermore the FE model predicts that all the material present deforms, as is assumed in the MT homogenization.

The composition consisting of only 70 volume percent of Al predicts an effective flowstress in the range of 20 to 30 Newton per square millimeter.

5. SECOND GENERATION OF FIRING MODELS

The first generation of firing models was developed to make physical sense on a product level and to predict residual stresses after firing of the silicon wafer [1]. The second generation of firing models presented in this article extends the description of the first generation of firing models by adding a detailed description of: the BSF, eutectic and Al bulk. To achieve these goals the BSF, eutectic and Al bulk layers are modeled individually. For the BSF and eutectic layers isotropic elastic plastic material behavior is used and for the Al layer the MT and FE homogenization strategies are used. The use of homogenization models to describe the Al bulk layer results in a precise prediction of the Al bulk response and a realistic prediction of the stresses present in the Al bulk layer. Furthermore isotropic elastic material behaviour is used to approximate the multi-crystalline silicon wafer behaviour and an isotropic elastic plastic

material behaviour is used for the silver fingers and bus-bars. The mechanical contribution of the silicon nitride coating is not taken into account since this layer is very thin and assumed to have little or no effect on bowing. An overview of the model showing the front-side pattern is given in Figure 8.

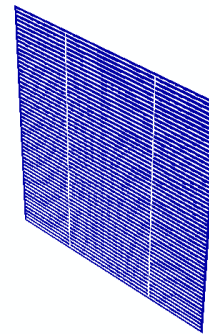


Figure 8: Overview of the three dimensional FE-model. The blue color is the silicon wafer and the white color the silver fingers and bus bars at the front-side. The Al on the back-side is not visible.

To model the firing process a number of process steps are followed as shown in Table 1.

Table 1: The steps used to model the firing process.

Step	Firing process
Step 1	Heat up silicon wafer to 800 degrees
Step 2	Add the silver finger elements. These elements represent the Ag fingers
	The BSF layer is set to grow
Step 3	Cool down to 660 degrees
	The BSF layer stops growing
	The elements representing the Al bulk/microstructure are added.
Step 4	Cool down to 570 degrees
	The elements representing the eutectic are added.
Step 5	Cool down to room temperature

The model predicts both bending and torque of the cells after firing. This is also seen in reality for very thin cells. In

Figure 9, a visual representation of the model results are given. The blue color is the silicon wafer and the white color the silver front-side metallization. 1) Shows the silicon wafer at the beginning of the simulation. 2) Shows the cell after the mechanical activation of the silver bus-bars and fingers. 5) Shows the results of the simulation process wherein the cell is cooled down to room temperature and the cell is bowed. Steps 3 and 4 are not shown as the amount of bowing induced by mechanical activation of the silver is insignificant.

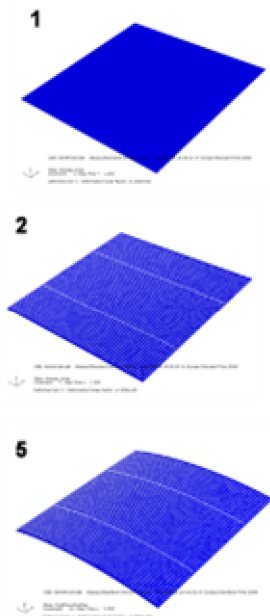


Figure 9: Images corresponding to the simulation steps of the firing process.

The results are shown in Figure 10 give an indication of the simulated cell torsion.



Figure 10: An image of the cell torque after the metallization process with a 120 micron wafer. The torsion can be observed by comparing the lower and upper edges of the cell. These two lines are not parallel. A similar torque was seen for processed wafers

The above results show that the model is able to qualitatively predict the bending and torque of the H-pattern cell after firing. The next step is to verify the model more quantitatively.

6. VERIFICATION

To get an indication of the quantitative predictability of the model two types of verification experiments were performed. The first verification was done by comparing the maximum bowing as

predicted by the model with bowing measured on cells with various thicknesses. The results are shown in Figure 11.

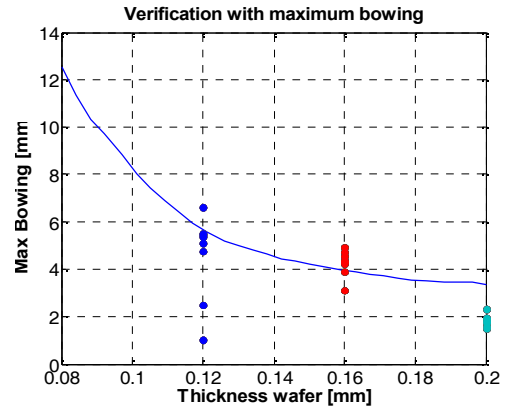


Figure 11: Verification of maximum bowing with respect to wafer thickness. The maximum bowing is plotted along the y-axis with respect to wafer thickness along the x-axis. The dotted points are measured values and the blue line is the result from a computer simulation

The second verification is done by comparing the shape of the bowed cell with the shape that the model predicts after the firing step. The bowed cell was measured using a Mahr Perthometer again for various cell thicknesses. This verification is shown in Figure 12 for a 200 µm cell. Other cell thicknesses show similar results

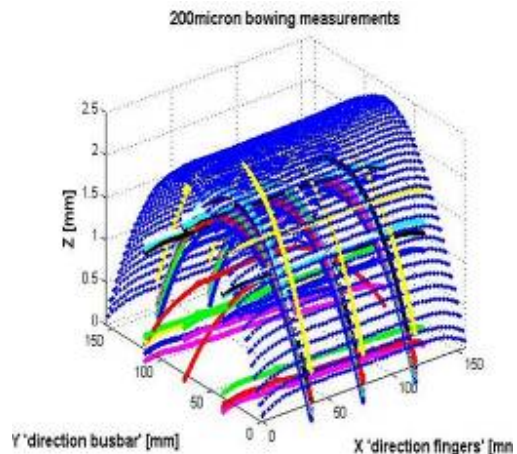


Figure 12: A direct verification between model results (in blue mesh) and measured data (colored lines). Only the direct verification of the 200 micron cell is shown. The purpose of these direct verification plots is to compare measured bowing to predicted bowing

7. PREDICTED ALUMINIUM COMPOSITION

In Figure 13 the correlation between cell bowing and the Al bulk effective flow stress is made.

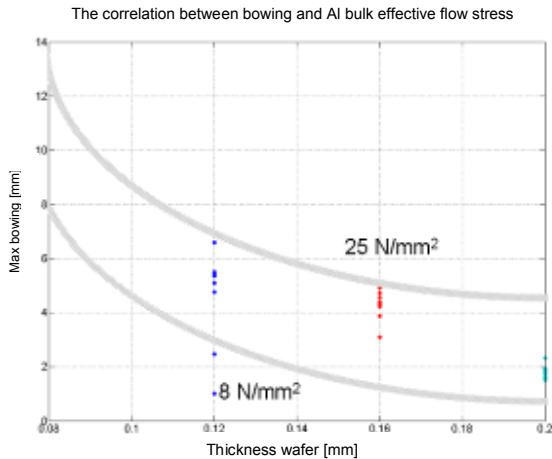


Figure 13: In this figure the measured bowing with respect to wafer thickness is shown also curves are plotted that indicate how much bowing can be expected as function of the effective flow stress.

The above figure shows that the Al bulk effective flow stress necessary for predicting the observed bowing is in the range of 8 to 25 Newton per square millimeter. In Table 2, the predicted effective flow stress ranges for the Al bulk compositions consisting of only Al are shown.

Table 2: Predicted effective flow stress ranges for microstructure compositions consisting of only Al.

Composition	Effective flowstress [N/mm ²]
40 volume percent Al	5-7
55 volume percent Al	6-15
70 volume percent Al	20-30

To predict the measured bowing an effective flow stress in the range of 8 to 25 Newton per square millimeter is needed in the Al bulk layer. This 8 to 25 Newton per square millimeter of effective flow stress is only predicted by Al bulk compositions consisting of only Al with a volume fraction of at least 40 percent. In short, the measured bowing in combination with the simulations indicates that the Al bulk will mostly consist of Al.

8. VOLUME FRACTION MEASUREMENTS

In Figure 14 a computed tomography analysis is shown of the Al bulk. The computed tomography analysis

shows that there is only a minimal amount of bismuth glass present.

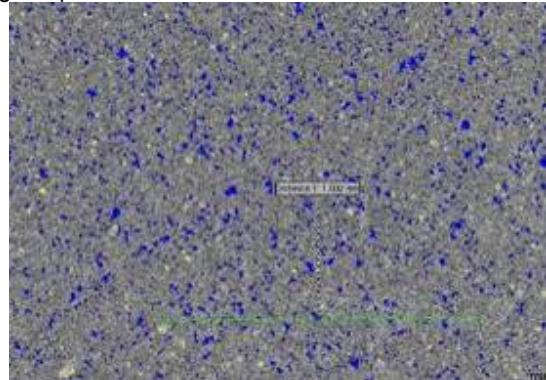


Figure 14: Computed tomography of an Al paste showing that Al (gray) and pores (blue) dominates the composition and that only a few percent of bismuth glass (yellow) is present.

In conclusion, both the computed tomography and the bowing and microstructure simulations indicate low bismuth glass content.

9. CONCLUSIONS & OUTLOOK

The effective yield stress has been predicted from:

- A finite element bowing model which calculated an 8-25 N/mm² effective flow stress; this is much lower than solid Al
- A homogenization microstructure model which calculated 55-70 vol. % of Al on the bases of the firing model.

The accuracy of the bowing predictions depends on many variables. Many of those variables such as wafer thickness and elastic modulus of the silicon can be directly measured. Some of those variables such as the effective flow stress in the Al bulk cannot be directly measured and simulations to predict the effective flow stress are necessary.

In future work the homogenization models will be directly implemented into the firing model as a material definition hereby predicting the effective flow stress more accurately and consequently to make more accurate bowing predictions possible.

The mechanical behaviour of the Al bulk layer can be predicted using homogenization strategies. The most accurate strategy is the finite element modelling strategy. The finite element strategy predicts a flow stress range significantly lower than that of solid Al for the simulated microstructures.

The mathematics used for building the models can also be used to describe ohmic behaviour, it is possible to use similar models to describe and explain the electrical behaviour of the Al bulk.

Silicon has a breaking strength of around 7000 Newton per square millimeter. It is shown in previous work that the breaking strength of a solar cell is considerably lower. The ratio between silicon breaking strength and that of a solar cell is caused by mechanical amplifiers. These amplifiers are measurable defects in the solar cell. The plan is to quantify these amplifiers in future work using modelling and measurements of the defects.

Finally it becomes possible with the use of the presented models to start designing an ideal firing process. For example a maximum allowable bowing can be assumed. This maximum bowing can be related by using the firing model to determine certain requirements on cell geometry and material behaviour. Also the maximum allowable effective flow stress in the Al bulk can be determined. This effective flow stress can be used to set up micro structural requirements for the Al bulk layer by using the homogenization methods. The question then becomes whether these requirements for an ideal firing process can be achieved practically.

ACKNOWLEDGEMENTS

The authors would like to thank ABAQUS Benelux BV and e-Xstream engineering for their assistance with the development of the models used in this work.

REFERENCES

- [1] T. van Amstel, I Bennett, 'Towards a better understanding of the thermo-mechanical behavior of H-pattern cells during metallization', proceedings of the 33rd International Photovoltaic Specialist Conference and Exhibition, San Diego, 11-16 May 2008.
- [2] P. Löfgen, 'Surface and volume recombination in silicon solar cells', PhD. Thesis, University of Utrecht, 1995
- [3] V.A. Popovich, T. van Amstel, I. J. Bennett, M. Janssen, I.M. Richardson, 'Microstructural and mechanical characterisation of aluminium back-contact layers and its application to thermomechanical multiscale modelling of solar cells', IEEE, 2009